Gas content and star formation efficiency in cosmic filaments

P.I.: Pascale Jablonka

Scientific context

It is now well known that environment is a main parameter of galaxy evolution, and in particular of star formation. In their empirical study, Peng et al (2010) show how the red fraction in galaxies from SDSS is a regular function of two parameters, the stellar mass, and the environmental density. Even in the field, massive galaxies, with M_* larger than 10^{11} $M_\odot$ are red and dead, while even dwarf galaxies of $M_* = 10^9$ $M_\odot$ are red when the overdensity of galaxies $\delta\rho/\rho$ is larger than 2.5×10^2. However, despite the clear empirical evidence for intrinsic and environmental quenching of star formation, the physical processes underlying these correlations are not well known. On one hand, intrinsic processes may include an ejection or heating of the gas through supernovae or AGN feedback (e.g. Springel et al. 2005; Croton et al. 2006) or the shock heating of the gas as it enters a massive halo (Dekel & Birnboim 2006). On the other hand environmental processes may remove gas through tidal heating and stripping that can occur in gravitational interactions and mergers between galaxies (Merritt 1983, Moore et al 1998), ram-pressure stripping due to the hot intra-cluster gas (Gunn & Gott 1972), or a decoupling from the cold gas supply accreting from the cosmic web (Larson, et al. 1980).

In a galaxy cluster, all of these mechanisms are certainly playing a role.

This process could be fast, at the entrance of spiral galaxies in the cluster, as shown by spectacular cases where more molecular gas is found in the ram-pressure tail than in the galaxy (e.g. Jachym et al 2014). In the tail, which is visible in both X-rays and Hα emission, the star formation efficiency is much lower than in normal galaxy disks. The molecular to atomic gas ratio is compatible to what is predicted from the observed pressure, when ram-pressure is added (Krumholz et al 2009).

The deficiency in atomic gas for galaxies in clusters has now been firmly established (e.g. Chung et al 2009), and molecular gas is also depleted as shown by several studies (Casoli et al., 1998; Lavezzi & Dickey, 1998; Vollmer et al 2008, Scott et al., 2013). The gas deficiency can be investigated at higher redshift only for molecular gas, with CO tracers, and we have indeed detected a few galaxies in clusters at z=0.4 and z=0.5, with a lack of CO emission relative to their infrared luminosity (Jablonka et al 2013). This suggests that molecular gas can be stripped before the star formation rate is affected. Combining all detections in clusters at intermediate redshifts, there is some trend for a decrease in CO towards the cluster centers.

Large galaxy redshift surveys have revealed that galaxies are distributed in a complex network of matter with a large dynamic range of local density, called the cosmic web or filamentary structures (Kitaura et al., 2009, Darvish et al. 2014). It is now interesting to know how galaxy evolution is affected at each local density.

Exploring different environments

It has been realized that a large part of cluster galaxy properties might have been acquired already before their entry in over-dense environments, while they belong to small groups, or cosmic filaments (e.g. Poggianti et al 1999, Cortese et al 2006). Due to the lower relative velocity in groups and filaments, galaxies can be more easily tidally stripped, and also experiment morphology transformation due to interactions and mergers. Also the environment may affect galaxies significantly earlier than the time when they have crossed the cluster virial radius. The star-forming fraction of galaxies declines and models predict systematic depletion of both hot and cold gas as far out as ∼5 virial radii (R_{200}) from the host center (Lewis et al. 2002; Bahé et al., 2013). The present project proposes to explore the physical properties of galaxies in cosmic filaments around the Virgo cluster, which have not yet been studied.

Our approach differs from and complements previous works, as it moves away from the simple field/group/cluster trilogy. We follow instead the complex network of galaxies around a well studied cluster.

The study of these filaments will benefit from the comparison with the rich ensemble of data, already obtained for Virgo: the atomic gas with the VLA by Chung et al (2009), and also at large scale with ALFALFA (Giovanelli et al 2005), the dust content with Herschel and HeViCS (Davies et al 2010), the optical with the NGVS survey (Ferrarese et al 2012), the UV data with GALEX GUViCS survey (Boselli et al 2011). While the star formation has been obtained with Hα and the FIR observations, the molecular

content has been obtained first with FCRAO (Kenney & Young 1989), and then IRAM data (Vollmer et al, 2005, 2008, and for the early-types Combes et al 2007, Young et al 2011).

The North-East filament

We selected the most contrasted and longest filament existing around Virgo. It is relatively straight over 20Mpc and extends up to 7 virial radii from the cluster center. Part of this filament is included in the Extended Virgo Cluster Catalog (EVCC) covering 725 deg^2 or 60 Mpc^2. The EVCC is about 5 times larger than the surface of Virgo proper, and extend to 3.5 virial radii. Half of the galaxis already benefit from HI data.

Our project is supported by a wealth of existing data which will enable detailed global analysis: SDSS u, g, r,i, and z imaging, optical spectroscopy, far infrared (WISE and/or IRAS) fluxes, leading to an accurate estimate of the galaxy stellar masses, as well as a clear census of the stellar population properties. HI masses are also already available as mentioned above **The rest of them will be gathered at ???**. In a companion proposal, we will gather very detailed Hα maps at CFHT, which shall reveal the status and spatial distribution of the hot gas. For the first time along a large scale structure, we shall be able to link all stages of the gas in galaxies and trace their evolution, both in terms of global content and spatial distribution, looking for possible depletion, evidence of stripping, specific orientation with respect to the direction of filament, relation with the cluster centric distance.

Note that Virgo is the closest relatively massive cluster. There is no counterpart in which the major question of the origin of star formation quenching could be addressed in such exquisite details.

Observating strategy

Our 20 targets evenly sample the infall path of galaxies to the center of Virgo. They share very similar velocities, from 2400 to 2800km/s, ensuring that they belong to the same filament, at a distance of 37 Mpc. We restricted the stellar mass range to between 10^9 and 10^{10} $M_\odot$ to allow proper comparison between galaxies, and requested 22μm WISE detection with SNR larger than 4 to secure detection in CO. These 20 selected galaxies are plotted on the sky plane in Figure 2 (left), and their properties listed in Table 1. Their morphologies are displayed in Figure 2 (right).

The specific CO observations of our 20 targets will serve the following immediate goals:

• determine their total molecular gas content. Note that the EMIR half power beam width will be ∼22arcsec, sometimes smaller than our galaxy sizes. We shall map the largest and strongest of our sources with 3 to 4 pointings (our time estimate are conservative ones to allow such flexibility). The most promising galaxies will be later map at high resolution with NOEMA. • Get insight in the gas excitation, through the CO(2-1)/CO(1-0) ratio, • Compare the molecular content to the star formation rate, obtained from both infrared and Hα fluxes (sdss spectra), and hence determine the star formation efficiency. This will serve direct comparison with the Virgo cluster and the field, using published analogous studies.

Technical justification

All our sources have velocities around 2500 km/s, and the CO(1-0) and CO(2-1) lines can be observed simultaneously at 2.6 mm and 1.3 mm with the E0/E2 configuration of EMIR in tracked WSW observing mode. With its 4GHz bandwidth, WILMA can cover all your sources from 2400 to 2800km/s, hence a single receiver tuning will be adequate for all your targets.

From the fluxes predicted in the two lines in Table 1, we can expect at least CO(1-0) antennae temperatures of $\sim$ 11mK, assuming a velocity width of 300 km/s. A velocity resolution of 20km/s will provide an excellent sampling, we aim at a minimum signal-to-noise ratio of 4, corresponding to a noise level of 2.9mK. For a typical elevation of 45.0 degrees, an observing frequency of 114.3 GHz and a spectrometer resolution of 20.0 km/s, the sensitivity estimator indicates that we will reach a sensitivity of 2.9 mK[Ta*] in 1.5 hr with average conditions (7.0 mm of pwv, Tsys 251.8 K[Ta*] mean per pixel). At 228.6 GHz (CO(2-1)), in the same amount of time, the noise level will reach 3.4mK, very similar to the CO(1-0), which will allow to detect both lines, even if they are somewhat subthermally excited. This will give very helpful insight in the gas excitation.

The 1.5h per source already takes into account pointing, focus, calibration and instrumental deadtimes. In conclusion, our 20 sources can be observed in 30 hours, with expected signal-to-noise ratios between 4 and 30, in three periods of 10h, between LST = 8h and 18h.

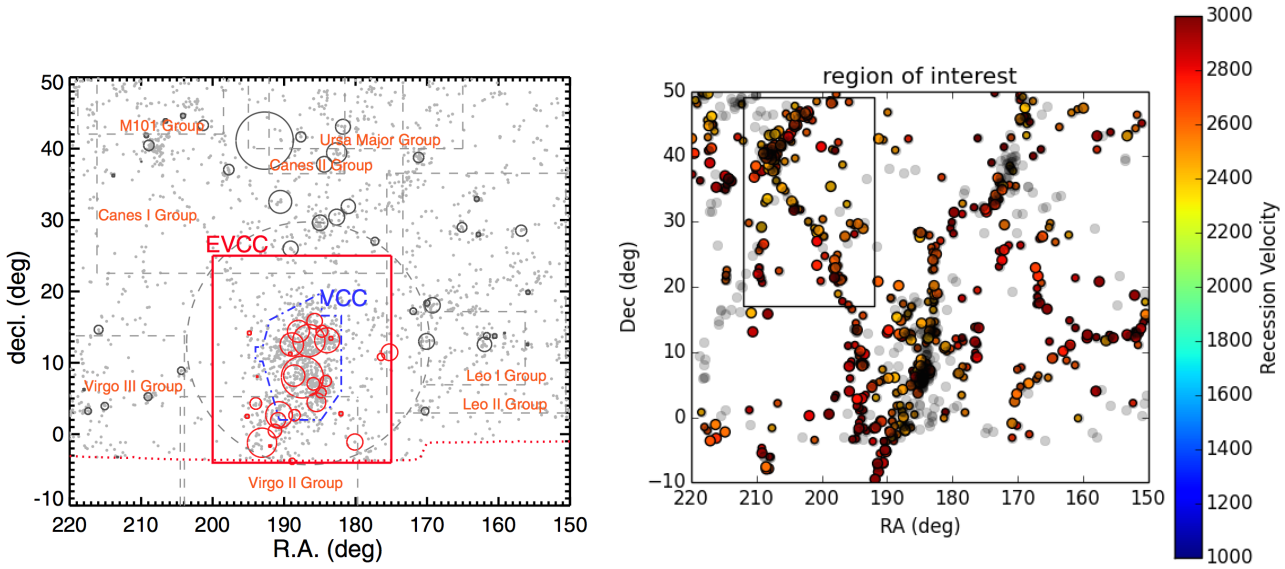

Figure 1: **Left** Distribution of galaxies in the Virgo cluster (blue dash contours), the externded catalog (EVCC, red) from Kim et al (2014), and all galaxies that can be identified in the SDSS, with velocities lower than 3000km/s. **Right** All WISE-detected sources in the Virgo environment. Those with velocities less than 2400km/s are plotted in gray to highlight the filament galaxies at a common velocity.

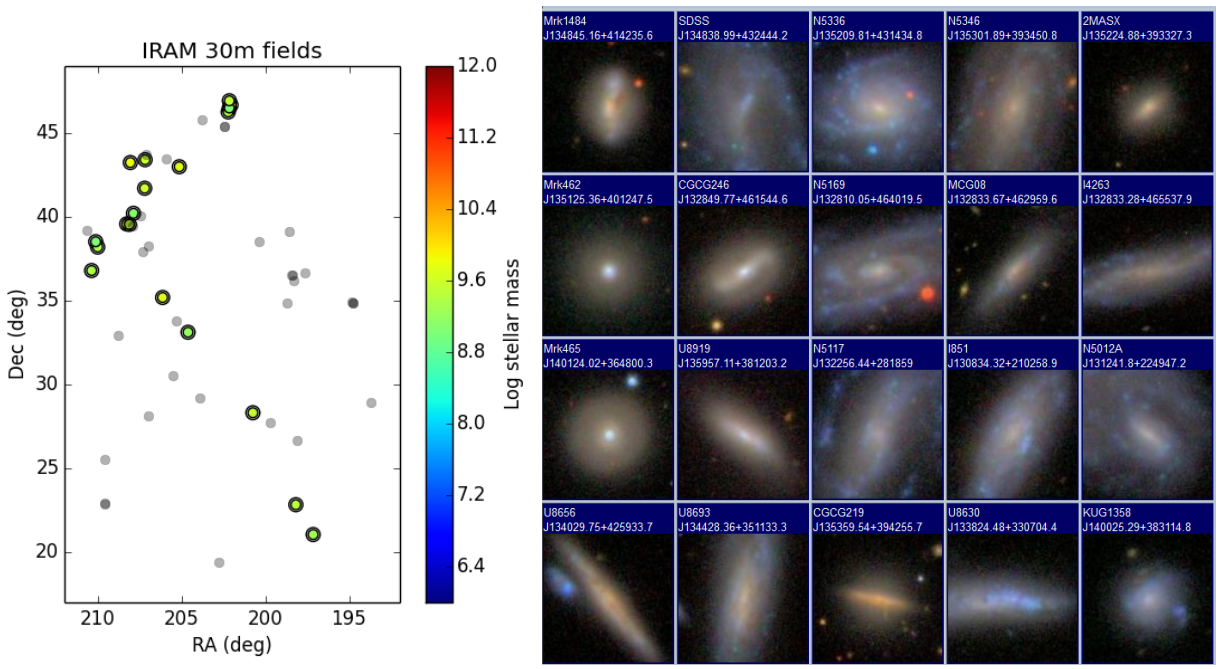

Figure 2: **Left** Our selected targets in the NE filament are plotted here, color-coded by their stellar mass. These were selected from among the ensemble of sources, with 2400 < V < 3000 km/s, to have stellar masses between 10^9 and 10^{10} $M_\odot$ and a 22μm detection with SNR larger than 4. **Right** SDSS images of our 20 targets. Each box is 50 arcsec in size.

Table 1: Definition of the sample, predicted CO(1-0) fluxes

Source	Name	Type	V	SFR	S(CO)	ν	log M(HI)
JRA+DEC			km/s	$M_\odot$/yr	Jy km/s	GHz	$M_\odot$
J134845.16+414235.3	Mrk1484	SPair	2677.5	0.43	92.1	114.251	–
J134835.47+432428.8	SDSS	Sm?	2447.2	0.02	15.7	114.338	–
J135209.79+431434.6	N5336	Scd	2416.1	0.19	89.9	114.350	9.46
J135301.89+393450.8	N5346	Scd	2532.5	0.02	13.4	114.306	9.19
J135224.87+393327.4	2MASX	SO/a	2734.9	0.10	30.4	114.229	–
J135125.37+401247.7	Mrk462	S	2508.1	0.26	63.5	114.315	–
J132849.76+461544.6	CGCG246-005	S	2678.8	0.07	26.2	114.250	–
J132810.05+464019.7	N5169	SBb	2524.9	0.19	72.0	114.309	9.65
J132833.65+462959.7	MCG08-25-006	S?	2635.0	0.06	24.3	114.267	–
J132833.19+465537.8	I4263	SBd	2757.9	0.02	12.3	114.220	9.40
J140124.02+364800.3	Mrk465	S	2691.3	0.35	66.0	114.246	–
J135957.09+381203.3	U8919	S	2710.9	0.04	17.6	114.238	–
J132256.47+281859.1	N5117	SBcd	2428.3	0.10	61.6	114.345	9.63
J130834.27+210259.9	I851	S	2622.8	0.25	80.0	114.271	9.48
J131241.78+224947.2	N5012A	SmPair	2548.7	0.14	71.0	114.299	9.44
J134031.19+425938.0	U8656	S?	2837.6	0.13	33.4	114.190	–
J134428.40+351131.9	U8693	S	2468.0	0.04	22.3	114.330	9.36
J135359.49+394256.0	CGCG219-021	S	2626.0	0.02	14.4	114.270	–
J133825.19+330702.9	U8630	S	2466.2	0.21	87.1	114.331	9.68
J140025.00+383113.0	KUG1358+387	S	2630.0	0.03	15.1	114.269	–

References

• Bahé Y.M., McCarthy, I.G., Balogh, M.L., Font, A.S.: 2013, MNRAS, 430, 3017 • Boselli A., Boissier S., Heinis S. et al.: 2011, A&A 528, 107 • Casoli F., Sauty S., Gerin M., et al.: 1998, A&A 331, 451 • Chung, A., van Gorkom, J. H., Kenney, J. D. P. et al.: 2009, AJ 138, 1741 • Combes F., Young L., Bureau M.: 2007, MNRAS 377, 1795 • Cortese L. Gavazzi, G.; Boselli, A. et al.: 2006 A&A 453, 847 • Croton D. Springel, V., White, S. D. M. et al.; 2006 MNRAS 365, 11 • Darvish B., Sobral, D., Mobasher, B. et al. 2014, ApJ, 796, 51 • Davies J., Baes M., Bendo G et al.: 2010, A&A 518, L48 • Dekel A., Birnboim Y.: 2006 MNRAS 368, 2 • Ferrarese L., Cote P., Cuillandre J-C. et al.: 2012 ApJS 200, 4 • Giovanelli R., Haynes M., Kent B.R. et al.: 2005 AJ 130, 2598 • Gunn, J. E. & Gott, J. R. I.: 1972, ApJ, 176, 1 • Jablonka P., Combes F., Rines K. et al.: 2013 A&A 557, A103 • Jachym P., Combes, F., Cortese, L. et al.: 2014, ApJ 792, 11 • Kenney J., Young J.: 1989, ApJ 344, 171 • Kim S., Rey S-C., Jerjen H. et al.: 2014, ApJS 215, 22 • Kitaura F, Jasche, J., Li, C. et al., 2009, MNRAS 400, 183 • Krumholz M., McKee, C. F., Tumlinson, J.: 2009 ApJ 693, 216 • Larson, R., Tinsley, B., Caldwell, N.: 1980, ApJ, 237, 692 • Lavezzi T.E., Dickey J.M., 1998, AJ 115, 405 • Lewis I., Balogh, M., De Propris, R. et al. 2002, MNRAS, 334, 673 • Merritt, D.: 1983, ApJ 264, 24 • Moore B., Lake G., Katz N.: 1998 ApJ 495, 139 • Peng, Y-J., Lilly S.J., Kovac K. et al.: 2010, Apj 721, 193 • Poggianti, B. M., Smail, I., Dressler, A. et al.: 1999 ApJ 518, 576 • Scott T.C., Usero A., Brinks E. et al.: 2013, MNRAS 429, 221 • Springel, V. et al.: 2005, ApJL, 620, L79 • Vollmer, B., Braine J., Combes F., Sofue Y.: 2005, A&A 441, 473 • Vollmer, B., Braine, J., Pappalardo, C., Hily-Blant, P.: 2008, A&A 491, 455 • Young, L., Bureau M., Davis T. et al.: 2011, MNRAS 414, 940